Arsenic Localization, Speciation, and Co-Occurrence with Iron on Rice (*Oryza sativa* L.) Roots Having Variable Fe Coatings

ANGELIA L. SEYFFERTH,[†] SAMUEL M. WEBB,[‡] JOY C. ANDREWS,[‡] AND SCOTT FENDORF*,[†]

Department of Environmental Earth Systems Science, Stanford University, Stanford, California, 94305, and Stanford Synchrotron Radiation Lightsource, SLAC National Accelerator Laboratory, Menlo Park, California 94025

Received April 9, 2010. Revised manuscript received September 10, 2010. Accepted September 14, 2010.

Arsenic contamination of rice is widespread, but the rhizosphere processes influencing arsenic attenuation remain unresolved. In particular, the formation of Fe plaque around rice roots is thought to be an important barrier to As uptake, but the relative importance of this mechanism is not well characterized. Here we elucidate the colocalization of As species and Fe on rice roots with variable Fe coatings; we used a combination of techniques—X-ray fluorescence imaging, μXANES, transmission X-ray microscopy, and tomography—for this purpose. Two dominant As species were observed in fine roots-inorganic As(V) and As(III) -with minor amounts of dimethylarsinic acid (DMA) and arsenic *tris*glutathione ($AsGlu_3$). Our investigation shows that variable Fe plaque formation affects As entry into rice roots. In roots with Fe plaque, As and Fe were strongly colocated around the root; however, maximal As and Fe were dissociated and did not encapsulate roots that had minimal Fe plaque. Moreover, As was not exclusively associated with Fe plaque in the rice root system; Fe plaque does not coat many of the young roots or the younger portion of mature roots. Young, fine roots, important for solute uptake, have little to no iron plaque. Thus, Fe plaque does not directly intercept (and hence restrict) As supply to and uptake by rice roots but rather serves as a bulk scavenger of As predominantly near the root base.

Introduction

Arsenic (As) is a human carcinogen and natural contaminant of soils worldwide, but in South and Southeastern Asia it is a catastrophic groundwater contaminant (*1*). While arsenic exposure via drinking water is well-documented (*2*−*5*), we are only beginning to understand the magnitude of chronic arsenic exposure from contaminated food products like rice (*Oryza sativa* L.). Upon soil flooding during rice cultivation, arsenic in soil is mobilized, taken up by roots, and accumulates in the edible portion of the grains. Rice grains from the U.S., France, and Japan contain up to 0.25, 0.23, and 0.18 μg As g^{-1}, respectively (*6*), and can be as high as 2 μg As g^{-1} in locations where contaminated groundwater is used for irrigation (e.g., Bangladesh) (*7, 8*). By consuming rice grains with arsenic present at levels of only 0.10 μg g^{-1}, the allowable daily arsenic intake will be exceeded for most rice sustenance diets (*7*−*9*). To reduce arsenic accumulation in rice grains, and thus human exposure, it is imperative to fully understand the basic mechanisms governing As accumulation in rice.

Physiological studies of As uptake by plant roots have indicated two main mechanisms of As entry into roots, which depend on the speciation (i.e., oxidation state) of As. Inorganic As(V) ($As(V)_i$) is a phosphate analog and is taken up into the root symplast by phosphate transport proteins in an active process (*10, 11*). Inorganic As(III) ($As(III)_i$), present in soil solution as $H_3AsO_3^0$ (pH < 8), shares the silicic acid (H_4SiO_4) transport system in rice through plant aquaporin channels located on root plasma membranes (*12*). Aquaporin channels transport water and other small, neutral molecules (e.g., arsenous acid, silicic acid) into the root symplast (*13, 14*). While our understanding of these transport pathways has advanced, it remains unclear which of these mechanisms prevails in rice paddy systems due to the complex processes that occur as As is transported from anoxic pore water to the oxygenated rhizosphere.

In aerated soil, arsenic typically resides as $As(V)_i$, which has a strong affinity for soil minerals, thus rendering it relatively immobile (*15*). However, upon flooding, soil-bound As becomes mobilized by reductive dissolution of iron(III) oxides (used here to collectively refer to hydroxides, oxyhydroxides, and oxides) and $As(V)_i$, leading to a predominance of $As(III)_i$ and reduced Fe(II) in bulk pore water of rice paddy soils (*16*). As rice plants deliver oxygen to roots via aerenchyma, O_2 diffuses to the rhizosphere and dissolved Fe(II) may be oxidized and precipitate on the exterior of rice roots (*17, 18*). The "iron plaque" may sorb As and limit its uptake into roots (*19, 20*). $Arsenic(III)_i$ is transported toward roots with transpirational water flux but it may be oxidized, at least partially, to $As(V)_i$ in the rhizosphere. $Arsenic(V)_i$ may compete with phosphate for uptake by roots, or for sorption onto ferric iron plaque (*10, 21*). Recent work has suggested that other solutes (e.g., nitrate, ammonium) may influence Fe cycling, and thus As uptake availability, in the rhizosphere of rice plants (*22*). Thus, root uptake of As in rice paddy systems depends on a balance of several factors, inclusive of the oxygenation capacity of rice roots, the extent and distribution of Fe(III) oxides, N supply, the relative abundance of $As(V)_i$ and P, the relative abundance of $As(III)_i$ and silicic acid, and the relative rates of transpiration and $As(III)_i$ oxidation.

While the presence of Fe plaque may limit root absorption of $As(V)_i$, the absence of Fe plaque may enhance absorption; however, the distribution of Fe plaque and its effect on root absorption of arsenic species is not well characterized. Moreover, little is known about the importance of young, fine roots verses mature, thick roots on iron plaque formation and, consequently, on As uptake and localization in rice roots. Fine roots, inclusive of root hairs, are generally younger and are more active in nutrient uptake than thick, lignified, mature roots where nutrient absorption is relatively low (*23*). The purpose of this investigation was to determine the distribution of Fe(III) (hydr)oxides on both thick and fine soil-grown rice roots and to determine the associated localization of As species in order to evaluate the role of Fe plaque in As attenuation.

* Corresponding author phone: (650) 723-5238; fax: (650) 725-2199; e-mail: fendorf@stanford.edu.
[†] Stanford University.
[‡] SLAC National Accelerator Laboratory.

10.1021/es101139z

Published on Web 10/11/2010

Experimental Section

Plant Growth and Root Samples. Root samples were obtained from rice grown in artificially As-contaminated soil and irrigated with As-contaminated water. Soil was obtained from the B_w horizon of Kohala series from the Big Island of Hawai'i that initially contained no detectable As. This soil was chosen to represent a highly weathered tropical soil that was low in dissolved silicic acid, allowing us to focus on the role of iron plaque on arsenic uptake; it contained 3.0 (±0.5) wt % acid ammonium oxalate-extractable Fe and had a pH of 5.95. Full details of growth parameters, soil-spiking procedures, and pore water monitoring can be found in the Supporting Information (SI). Pore water chemistry in the pots was monitored with Rhizon samplers (Soil Moisture Corp.). Irrigation water contained 300 μg/L in an 80/20 mixture of $As(III)_i/As(V)_i$ to reflect typical contaminated groundwater used during dry-season irrigation in South and Southeast Asia (see ref *24*). After seedling emergence, plants were thinned to three seedlings per pot.

Approximately 6 weeks post transplantation (vegetative growth stage), one plant's root system was carefully removed from the center of the pot by hand-digging around the base of the plant. The root mass was gently hand washed with DDI water to remove soil particles and allowed to dry anaerobically (96% N_2/4% H_2) in a glovebag. A fine lateral root was removed from a larger root under magnification and mounted onto the end of a support rod for transmission X-ray microscopic imaging (TXM), nanotomography, X-ray fluorescence (XRF) imaging, and μ-X-ray absorption near-edge spectroscopy (μXANES).

The remaining plants were grown to maturity and harvested after grain filling. Plants were cut approximately 4 cm above the soil surface, and the entire root mass was removed from the soil and rinsed and dried anaerobically as described above. Intact roots, still attached to the shoot base, were used for optical and XRF imaging. A single root approximately 1 mm in diameter that showed an abrupt transition from white to red color (low and high degree of Fe plaque pigmentation) was obtained from the center of the pot and utilized for X-ray tomography.

XRF Imaging of Rice Root System. XRF imaging of the roots was conducted at Stanford Synchrotron Radiation Lightsource (SSRL) beamline 10−2, optimized for continuous-scanning, large-aperture XRF imaging. X-ray tomography was also conducted at beamline 10−2 on the root showing an abrupt transition from low to high degree of pigmentation. Chemical speciation images were obtained by imaging at four energies: 11 880, 11 874, 11 871, and 11 865 eV and performing a least-squares fit of the images to normalized mu of several As standards. Full details of the XRF imaging parameters can be found in the SI.

Transmission X-ray Microscopic (TXM) Imaging and Microtomography. A section of the fine lateral root tip described above was imaged at beamline 6−2c at SSRL equipped with an Xradia transmission X-ray microscope instrument (*25*). Both two-dimensional (2D) raster-scanned absorption contrast images and three-dimensional (3D) nanotomographic images were obtained. Full details of the TXM imaging parameters can be found in the SI.

***μ*XRF Imaging and *μ*XANES.** The entire fine lateral root was further imaged at beamline 10.3.2 at the Advanced Light Source (ALS) of Lawrence Berkeley National Laboratory. The fine root was imaged at three energies: 11880, 11874, and 11871 eV and chemical speciation maps of total As, As(V), and As(III) were obtained by performing a least-squares fit of the images to normalized mu of standards. Full details of the XRF imaging parameters can be found in the SI. In addition to the element-specific images, As μXANES spectra were obtained at 6 locations along the root with maximum fluorescence intensities for total As (i.e., "hotspots").

Data Processing and Analysis. The SMAK program (*26*) was used to process fluorescence images of total Fe and total As in the rice root system as well as XRF tomographic and chemical speciation images of the differentially pigmented root. Chemical speciation maps of As(III) and As(V) as well as tricolor plots of As species and Fe associated with the fine root were created using ALS beamline 10.3.2 software. The SIXPACK program (*27*) was used for background subtraction, normalization, and linear combination fitting of As Kα

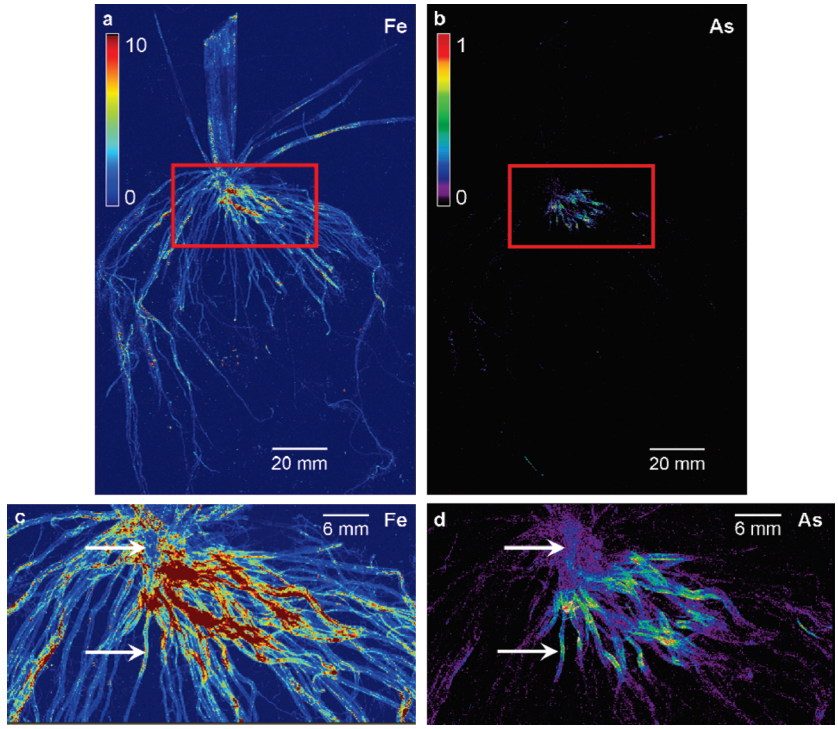

FIGURE 1. X-ray fluorescence images of Fe (a, c) and As (b, d) distributed within the rice root system. Images c and d represent magnified images of boxes in a and b, and the arrows represent areas where As is abundant while Fe is not.

μXANES spectra. Full details of fitting parameters and standards used can be found in the SI.

Results

Pore Water Chemistry and Final As Concentrations in Plant Parts. The pore-water pH increased slightly from 5.8 to 6.3, and the total dissolved Fe decreased from an initial increase of 1.3 mg L^{-1} to below detection throughout the growth period. During this time, total As decreased from 190 to 4 μg L^{-1} from day 11 to day 57, and then increased steadily to ca. 20 μg L^{-1}; $As(III)_i$ and $As(V)_i$ followed a similar trend and remained in roughly similar proportions to the initial input levels of 80% and 20% of the total As added in irrigation water. Dissolved Si increased slightly from 1.5 to 4 mg L^{-1} from day 11 to day 57, then decreased to <1 mg L^{-1}. Dissolved P decreased from 75 to 13 μg L^{-1} from day 11 to day 19 and then steadily increased to 73 μg L^{-1}. Total As concentrations of plant fractions (μg g^{-1} ± standard error, $n = 3$) were 0.344 (±0.021) in rice grains (unpolished), 0.409 (±0.077) in husks, 6.56 (±0.57) in leaves, 3.20 (±0.35) in stems, and 79.2 (±8.36) in roots. Note that the grain was unpolished when digested, and that any Fe coatings were left intact on roots prior to digestion.

Imaging of Entire Rice Root System. Optical images of rice roots obtained immediately after harvest illustrate pigmentation by Fe plaque (SI Figure 1). Upon visual inspection, some large roots are highly pigmented; however, many of the thick roots and especially the fine roots exhibit minimal Fe staining. XRF images obtained of the entire rice root system show both As and Fe present in many of the roots, with highest intensities near the shoot base but also relatively high intensities near the root tips (Figure 1a, b). Increased magnification of the area just below the shoot base illustrated co-occurrence of Fe and As (Figure 1c, d) in specific areas. However, areas of thick roots were observed where As was relatively abundant, whereas Fe was not (see white arrows on Figure 1c, d). It is clear that the highest arsenic fluorescence intensity does not strongly correlate with the highest iron fluorescence intensity (SI Figure 2a, b).

Computed X-ray tomographic images clearly show the relationship between As and Fe colocalization. When Fe plaque is visible (highly pigmented), total As is associated with Fe around the entire root section (Figure 2a, b). However, when Fe plaque is not visible (minimal pigmentation), total As and Fe show less colocalization and do not encompass the entire root section (Figure 2f, g). In the lesser-pigmented areas, As is concentrated in an area near the outer-edge of the root, approximately 250 μm from the highest concentration of Fe (Figure 2f, g). Arsenic speciation revealed that in both the highly and minimally pigmented root portions, arsenate is the dominant species in the most concentrated arsenic hotspots, with minor amounts of arsenite and $AsGlu_3$ (Figure 2c–j). In the root portion with minimal pigmentation, $AsGlu_3$ is the As species most associated with the Fe hotspots, whereas in the highly pigmented root portion, arsenate was the As species associated with the Fe 'hotspot' (Figure 2a, d, f, j).

TXM Imaging, Nanotomography, and μXANES of a Fine Root. The fine root was visualized using 2D absorption contrast TXM imaging (Figure 3a), with elemental composition deduced from X-ray microfluorescence imaging (Figure 4) (note that in addition to As and Fe, fluorescence of Zn, Cu, Cr, Ni, Ti, Ca, and K were monitored but were scarce in the root). The root tip has a higher abundance of As and Fe, whereas the area toward the root base has As and Fe accretions in more localized areas (Figure 3a). High-resolution 3D nanotomography obtained on two sections along the root, near the tip and toward the base, reveal internal accretions of As and Fe. Orthoslices (2D) of the 3D fine root reconstruction, two near the tip and two toward the root base

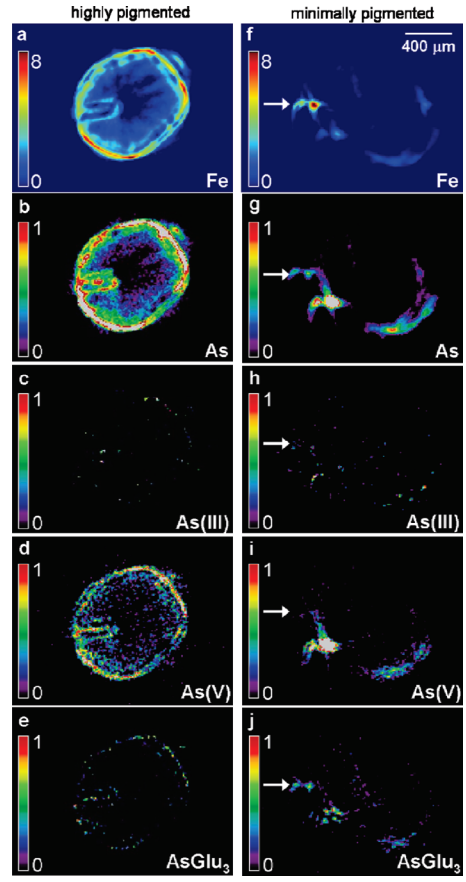

FIGURE 2. Cross-sectional computed X-ray tomography of the highly pigmented (a-e) and minimally pigmented portions (f–j) of a rice root showing spatial distribution of total Fe (a, f), total As (b, g), arsenite (c, h), arsenate (d, i), and arsenic *tris*glutathione (e, j). White arrow points to section of the minimally pigmented root corresponding to the Fe hotspot.

(Figure 3b), reveal smaller accretions of As and Fe more homogeneously distributed within the root tip (Figure 3b1 and b2), with larger accretions on the interior and exterior in patchy distribution near the root base (Figure 3b3 and b4).

XRF chemical speciation imaging of As, along with total Fe, show that total Fe and total As co-occur in the fine root sample (Figure 4a, b), in contrast to the As–Fe trend noted for the entire root mass (Figure 1). $Arsenic(V)_i$ and $As(III)_i$ co-occurred in localized hotspots but also occur independently of one another (Figure 4e). The largest difference in localization of As species was in the root tip, which was dominated by $As(III)_i$ with little $As(V)_i$ (Figure 4c, d, and SI Figure 3). XANES spectra obtained on six of these hotspots (Figure 4e) revealed major and minor As species with inflection points of ca. 11 874, 11 872, and 11 870.5 eV (SI Table 1). Linear combination fitting of the edge spectra reveal that 66–87% of the As was $As(V)_i$, while between 0 and 15% was $As(III)_i$; DMA accounted for 0–23%, while $AsGlu_3$ was present at trace levels in only two spots (SI Table 1).

Discussion

The concentration of arsenic in unpolished rice grain in our experiment (0.344 μg g^{-1}) was similar to levels reported in market-basket surveys from south-central United States (*8*) and Bangladesh (*28*), slightly higher than the "normal" worldwide range of 0.08–0.20 μg g^{-1} calculated by Zavala and Duxbury (*29*), and similar to those reported for soil-grown rice plants with significant Fe plaque coatings (*20*). The As levels in the husk (0.4 μg g^{-1}) were much lower than

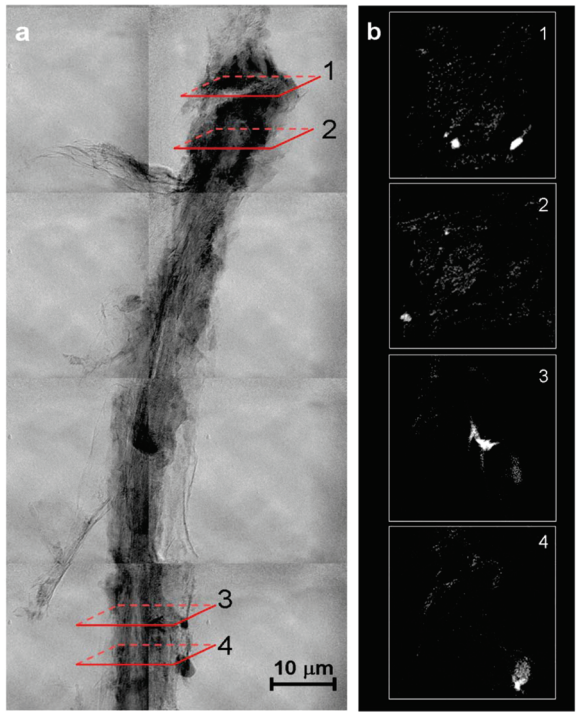

FIGURE 3. High-resolution absorption contrast image of a fine root (ca. 10 × 100 μm) at 5400 eV, where dark areas indicate highest absorption of the incident X-ray beam (a); sequential crosssectional orthoslices based on reconstructed tomographic images of the fine root from (a) in the areas indicated by boxes 1−4, where white areas indicate maximum absorption and are representative of As and Fe (b). Note that Figure 4 shows the Fe and As species fluorescence image for the same root, with the box in Figure 4a depicting the root tip imaged by TXM.

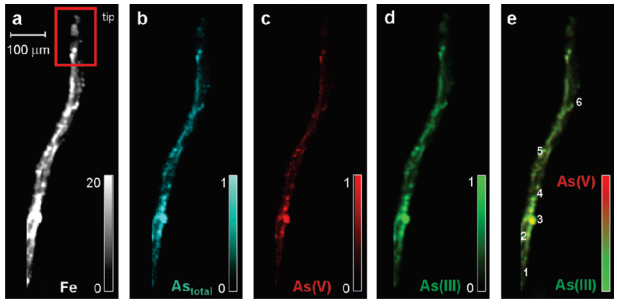

FIGURE 4. X-ray fluorescent images of total Fe (a) and total As (b); As(V) (c); As(III) (d); As(V); and As(III), numbers indicate areas where μXANES were obtained (e); red box in (a) shows where nanotomography (Figure 3) was obtained on the fine root tip.

that reported by Lombi et al. (*30*) but are comparable to other studies grown under similar soil conditions (*31*−*33*), which may reflect genotypic differences with respect to As translocation in plant fractions. The straw and root concentrations of <10 and 79 μg g^{-1}, respectively, were within the range of previous reports using similar growth conditions (*32, 34*).

Fe plaque formed preferentially on thick mature roots near the water−air interface with minimal Fe plaque on fine, young roots. These observations are similar to those of Chen et al. (*18*) who found thick iron coatings on mature roots and nonexistent iron coatings on young roots or on the young portion of older roots (i.e., root tips) in soil-grown rice plants. Young, fine roots, inclusive of root hairs, are more important for overall nutrient uptake than mature roots (*18, 23, 35*) and we hypothesize that fine roots may be important for net As accumulation in rice plants. Root tips, in particular, could be an important route of entry for As(III)$_i$ because the primary barrier to uptake into vascular tissue, the Casparian strip, is not well-defined in developing root tips (*36*) and As entering here has access to the metaxylem and thus transport to the shoot. The influx of As species from the axial to the basal regions of rice roots is currently unresolved.

Chen et al. (*37*) demonstrated that As(III)$_i$ uptake was enhanced by the presence of Fe plaque based on a 20 min uptake study of arsenate and arsenite on excised rice roots with and without iron plaque. The mechanism for enhanced As(III)$_i$ uptake is not clear but the authors suggest it is due to a labile As(III)$_i$ complex on the plaque. It is noteworthy to mention, however, that the increase in As(III)$_i$ influx with Fe plaque only occurred appreciably for the highest As concentration (0.107 mM As) in their experiments, whereas influx remained approximately steady or started to decrease from 0.0133 to 0.0533 mM As (*37*). An alternative hypothesis is that at their highest As concentrations, which may exceed values commonly observed in rice paddies, the Fe plaque was at surface site saturation, leading to increased As(III)$_i$ influx into the root.

In our study, roots with Fe coatings had arsenate associated with the plaque on the exterior of the root, with a partial exterior rim of arsenite (Figure 2c, d). Arsenate was associated with Fe on the interior of the root; it is not clear whether As entered as a mixture of As species, or was converted (oxidized) on the root interior. Xu et al. (*38*) showed rapid reduction of arsenate to arsenite after root As uptake in tomato plants, but, in contrast, we observed mostly arsenate on the root interior. These differences between As speciation in roots of tomato vs rice illustrate interspecies differences in As dynamics in planta. In our study, roots with limited Fe plaque were not coated with arsenic; instead, arsenic was concentrated in an area that was dissociated from Fe. In the absence of Fe plaque, both arsenate and arsenite may move freely into the apoplastic space. Because Fe plaque did not form appreciably on root portions important for solute uptake, the plaque-free uptake route may be significant in soil-grown rice plants with variable Fe plaque coatings.

Iron and arsenic co-occur most strongly on the roots closest to the water−air interface. Our findings are more than likely due to oxygenation of the upper root zone due to atmospheric oxygen diffusion, and/or that these roots are the oldest roots and thus have more time to accumulate Fe plaque. In either case, the root section with most Fe plaque is not the most active area for solute uptake, which correspond to the findings of Chen et al. (*18*). A smaller amount of Fe plaque coatings was present toward the younger portion of the root (SI Figure 1), which had only a small amount of associated As (Figure 1). As oxygen is transported to roots via aerenchyma, more oxygen is released where barriers to radial oxygen loss are minimal, such as in root tips and lateral roots (*39, 40*). Thus, these areas should have the greatest abundance of Fe plaque, but in our study lateral roots were minimally pigmented with Fe oxides and did not contain appreciable As in the coating. Moreover, root tips that contained moderate amounts of Fe (Figure 1) exhibited a patchy distribution of As and Fe in the interior (Figure 3). Tanaka et al. (*41*) showed that Fe was present on the root tip interior in rice, which corroborates with our findings. Near root tips and in lateral roots, where minimal barriers to uptake exist, As and Fe are absorbed, leading to less As(V) associated with Fe plaque. It is noteworthy that in another study of Fe plaque distribution on rice roots, Fe plaque formation was highest at root tips and lowest at the root base (*20*). These results contrast our results and might be due to genotypic differences with respect to oxidizing power of rice roots (*33*).

Our finding that As and Fe are not highly correlated in the entire rice root system is similar to those of Hansel et al. (*19*), who found that high levels of As do not always correspond to high levels of Fe in *Phalaris arundinacea* (reed canarygrass). They are, however, in contrast to Blute et al. (*42*) who found that Fe and As were highly correlated in *Typha Latifolia* (cattail) roots growing in an As contaminated site. These differences may be physiological (i.e., different rate of O_2 diffusion from aerenchyma) or chemical (i.e., different As and or Fe concentrations) in nature. Similar to Hansel et al. (*19*), we found evidence for As sequestration on the fine root interior (i.e., not exclusively on iron plaque), whereas Blute et al. (*42*) found As only on the root exterior and associated with Fe plaque. These results suggest that some aquatic plant roots may sequester As inside vacuoles (e.g., rice, reed canarygrass), whereas others do not (e.g., cattail). Another hypothesis is the roots analyzed in the various studies differed in the amount of Fe plaque and thus associated As (see, for example, Figure 2 of this study).

For arsenic not associated with the iron plaque, $As(V)_i$ and $As(III)_i$ species were dominant within fine roots, with a smaller amount of DMA and even less $AsGlu_3$. DMA could be microbiologically produced in the soil and then absorbed by fine roots, and it has been shown recently that the aquaporin channels responsible for $As(III)_i$ and H_4SiO_4 uptake also facilitate DMA and MMA translocation to the vascular tissue (*43*). DMA may also be produced in planta but direct evidence for inorganic to organic As transformation in planta is presently unresolved. Our results are similar to Pickering et al. (*44*) who found As(III) coordinated with oxygen and not thiolate groups in vacuoles of *Pteris vitatta* gametophytes, but are in contrast with As(III) coordinated with thiol groups in *Brassica junca* shoots (*45*). Webb et al. (*46*) showed As(III) coordinated with oxygen but also with thiol groups, the latter of which at high As concentrations. It is noteworthy that although $AsGlu_3$ was minimally present in the fine root, it was more evident in slightly larger roots (Figure 2e, j). Rice roots have been shown to reduce $As(V)_i$ to $As(III)_i$ in hydroponic culture (*38*), but sequestration with glutathione might be an intermediate step in this process (*44*). In any case, the organic arsenic forms are a minor proportion of the total arsenic within the roots.

Our study illustrates that variable Fe plaque coatings affect As behavior in rice roots. Roots with Fe plaque have $As(V)_i$ in strong colocalization, with an exterior coating of arsenite. However, the presence of $As(V)_i$ on the root interior (i.e., within the cellular structure of the root) indicates that $As(V)_i$ is not exclusively reduced to $As(III)_i$ or $AsGlu_3$ once on the root interior. In roots without Fe plaque, $As(V)_i$ and $As(III)_i$ have little restriction to apoplastic entry. Given the lack of Fe plaque in many of the roots, especially the fine roots, Fe plaque might not be an effective barrier to As uptake by rice roots (at least for systems with limited Fe(II) available for plaque formation).

Acknowledgments

We thank Florian Merier for assistance with sample mounting and data processing at SSRL beamline 6-2c and Yoko Masue-Slowey and Michael S. Massey for help with data collection. We also thank Matthew A. Marcus for assistance in conducting μXRF imaging and data processing on beamline 10.3.2 at ALS, and Oliver Chadwick for assistance with soil collection. Funding for this research was provided by the Stanford NSF Environmental Molecular Sciences Institute (NSF-CHE-0431425) and a NSF Minority Postdoctoral Fellowship (award no. 0905295) to A.L. Seyfferth. The TXM microscope has been supported by the National Institutes of Health (NIH)/National Institute of Biomedical Imaging and Bioengineering (NIBIB) grant number 5R01EB004321. SSRL and the ALS are supported by the Department of Energy, Office of Basic Energy Sciences.

Supporting Information Available

Detailed information about the spectroscopic imaging parameters and corresponding data analysis. Figure SI 1 is a photograph of the rice root system showing pigmentation from Fe plaque. Figure SI 2 shows an X-ray fluorescence image of Fe and As (a); and a correlation plot between Fe and As (b) from the root system from the box in Figure 2a and b (main manuscript). Figure SI 3 illustrated the correlation between $As(III)_i$ and $As(V)_i$ in the entire fine root and root tip. Additionally, Table SI 1 shows the inflection point of the binding energy and corresponding intensity for standard spectra and "hotspots" where XANES spectra were obtained on the fine root sample shown in Figure 4e (main manuscript) as well as results from linear combination fitting. This material is available free of charge via the Internet at http://pubs.acs.org.

Literature Cited

(1) Fendorf, S.; Michael, H. A.; van Geen, A. Spatial and temporal variations of groundwater arsenic in south and southeast Asia. *Science* **2010**, *328*, 1123–1127.
(2) Ahmed, M. F.; Ahuja, S.; Alauddin, M.; Hug, S. J.; Lloyd, J. R.; Pfaff, A.; Pichler, T.; Saltikov, C.; Stute, M.; van Geen, A. Ensuring safe drinking water in Bangladesh. *Science* **2006**, *314*, 1687–1688.
(3) Buschmann, J.; Berg, M.; Stengel, C.; Sampson, M. L. Arsenic and manganese contamination of drinking water resources in Cambodia: Coincidence of risk areas with low relief topography. *Environ. Sci. Technol.* **2007**, *41*, 2146–2152.
(4) Opar, A.; Pfaff, A.; Seddidue, A. A.; Ahmed, K. M.; Graziano, J. H.; van Geen, A. Responses of 6500 households to arsenic mitigation in Araihazar, Bangladesh. *Health Place* **2007**, *13*, 164–172.
(5) Yu, W. H.; Harvey, C. M.; Harvey, C. F. Arsenic in groundwater in Bangladesh: A geostatistical and epidemiological framework for evaluating health effects and potential remedies. *Water Resour. Res.* **2003**, *39*, 1146.
(6) Meharg, A. A.; Williams, P. N.; Adomako, E.; Lawgali, Y. Y.; Deacon, C.; Villada, A.; Cambell, R. C. J.; Sun, G.; Zhu, Y. G.; Feldmann, J.; Raab, A.; Zhao, F. J.; Islam, R.; Hossain, S.; Yanai, J. Geographical variation in total and inorganic arsenic content of polished (white) rice. *Environ. Sci. Technol.* **2009**, *43*, 1612–1617.
(7) Williams, P. N.; Price, A. H.; Raab, A.; Hossain, S. A.; Feldmann, J.; Meharg, A. A. Variation in arsenic speciation and concentration in paddy rice related to dietary exposure. *Environ. Sci. Technol.* **2005**, *39*, 5531–5540.
(8) Williams, P. N.; Raab, A.; Feldmann, J.; Meharg, A. A. Market basket survey shows elevated levels of as in South Central US processed rice compared to California: Consequences for human dietary exposure. *Environ. Sci. Technol.* **2007**, *41*, 2178–2183.
(9) Meharg, A. A.; Rahman, M. Arsenic contamination of Bangladesh paddy field soils: Implications for rice contribution to arsenic consumption. *Environ. Sci. Technol.* **2003**, *37*, 229–234.
(10) Meharg, A. A.; Macnair, M. R. Suppression of the high-affinity phosphate-uptake system - a mechanism of arsenate tolerance in *Holcus lanatus* L. *J. Exp. Bot.* **1992**, *43*, 519–524.
(11) Ullrich-Eberius, C. I.; Sanz, A.; Novacky, A. J. Evaluation of arsenate-associated and vanadate-associated changes of electrical membrane potential and phosphate transport in *Lemna gibba* G1. *J. Exp. Bot.* **1989**, *40*, 119–128.
(12) Ma, J. F.; Yamaji, N.; Mitani, N.; Xu, X.-Y.; Su, Y.-H.; McGrath, S. P.; Zhao, F.-J. Transporters of arsenite in rice and their role in arsenic accumulation in rice grain. *Proc. Natl. Acad. Sci. U.S.A.* **2008**, *105*, 9931–9935.
(13) Maurel, C.; Verdoucq, L.; Luu, D. T.; Santoni, V. Plant aquaporins: Membrane channels with multiple integrated functions. *Annu. Rev. Plant Biol.* **2008**, *59*, 595–624.
(14) Bansal, A.; Sankararamakrishnan, R. Homology modeling of major intrinsic proteins in rice, maize and Arabidopsis: comparative analysis of transmembrane helix association and aromatic/arginine selectivity filters. *BMC Struct. Biol.* **2007**, *7*.
(15) Bowell, R. J. Sorption of arsenic by iron oxides and oxyhydroxides in soils. *Appl. Geochem.* **1994**, *9*, 279–286.

(16) Xu, X. Y.; McGrath, S. P.; Meharg, A. A.; Zhao, F. J. Growing rice aerobically markedly decreases arsenic accumulation. *Environ. Sci. Technol.* **2008**, *42*, 5574–5579.
(17) Howeler, R. H. Iron-induced oranging disease of rice in relation to physicochemical changes in a flooded oxisol. *Soil Sci. Soc. Am. J.* **1973**, *37*, 898–903.
(18) Chen, C. C.; Dixon, J. B.; Turner, F. T. Iron coatings on rice roots—Morphology and models of development. *Soil Sci. Soc. Am. J.* **1980**, *44*, 1113–1119.
(19) Hansel, C. M.; La Force, M. J.; Fendorf, S.; Sutton, S. Spatial and temporal association of As and Fe species on aquatic plant roots. *Environ. Sci. Technol.* **2002**, *36*, 1988–1994.
(20) Liu, W. J.; Zhu, Y. G.; Hu, Y.; Williams, P. N.; Gault, A. G.; Meharg, A. A.; Charnock, J. M.; Smith, F. A. Arsenic sequestration in iron plaque, its accumulation and speciation in mature rice plants (*Oryza sativa* L.). *Environ. Sci. Technol.* **2006**, *40*, 5730–5736.
(21) Hossain, M. B.; Jahiruddin, M.; Loeppert, R. H.; Panaullah, G. M.; Islam, M. R.; Duxbury, J. M. The effects of iron plaque and phosphorus on yield and arsenic accumulation in rice. *Plant Soil* **2009**, *317*, 167–176.
(22) Chen, X. P.; Zhu, Y. G.; Hong, M. N.; Kappler, A.; Xu, Y. X. Effects of different forms of nitrogen fertilizers on arsenic uptake by rice plants. *Environ. Toxicol. Chem.* **2008**, *27*, 881–887.
(23) *Plant Solute Transport*. Yeo, A. R. , Flowers, T. J. , Eds.; Blackwell Publishing Ltd: Oxford, 2007.
(24) Roberts, L. C.; Hug, S. J.; Dittmar, J.; Voegelin, A.; Saha, G. C.; Ali, M. A.; Badruzzanian, A. B. M.; Kretzschmar, R. Spatial distribution and temporal variability of arsenic in irrigated rice fields in Bangladesh. 1. Irrigation water. *Environ. Sci. Technol.* **2007**, *41*, 5960–5966.
(25) Tkachuk, A.; Duewer, F.; Cui, H. T.; Feser, M.; Wang, S.; Yun, W. B. X-ray computed tomography in Zernike phase contrast mode at 8 keV with 50 nm resolution using Cu rotating anode X-ray source. *Z. Kristallogr.* **2007**, *222*, 650–655.
(26) Webb, S. M. *SMAK: Sam's Microprobe Analysis Kit, V 0.46*; Stanford Synchrotron Radiation Laboratory: Stanford, CA, 2006.
(27) Webb, S. M. SIXpack: a graphical user interface for XAS analysis using IFEFFIT. *Phys. Scr.* **2005**, *T115*, 1011–1014.
(28) Williams, P. N.; Islam, M. R.; Adomako, E. E.; Raab, A.; Hossain, S. A.; Zhu, Y. G.; Feldmann, J.; Meharg, A. A. Increase in rice grain arsenic for regions of Bangladesh irrigating paddies with elevated arsenic in groundwaters. *Environ. Sci. Technol.* **2006**, *40*, 4903–4908.
(29) Zavala, Y. J.; Duxbury, J. M. Arsenic in rice: I. Estimating normal levels of total arsenic in rice grain. *Environ. Sci. Technol.* **2008**, *42*, 3856–3860.
(30) Lombi, E.; Scheckel, K. G.; Pallon, J.; Carey, A. M.; Zhu, Y. G.; Meharg, A. A. Speciation and distribution of arsenic and localization of nutrients in rice grains. *New Phytol.* **2009**, *184*, 193–201.
(31) Carey, A. M.; Scheckel, K. G.; Lombi, E.; Newville, M.; Choi, Y.; Norton, G. J.; Charnock, J. M.; Feldmann, J.; Price, A. H.; Meharg, A. A. Grain unloading of arsenic species in rice. *Plant Physiol.* **2010**, *152*, 309–319.
(32) Abedin, M. J.; Cotter-Howells, J.; Meharg, A. A. Arsenic uptake and accumulation in rice (*Oryza sativa* L.) irrigated with contaminated water. *Plant Soil* **2002**, *240*, 311–319.
(33) Mei, X. Q.; Ye, Z. H.; Wong, M. H. The relationship of root porosity and radial oxygen loss on arsenic tolerance and uptake in rice grains and straw. *Environ. Pollut.* **2009**, *157*, 2550–2557.
(34) Abedin, M. J.; Cresser, M. S.; Meharg, A. A.; Feldmann, J.; Cotter-Howells, J. Arsenic accumulation and metabolism in rice (*Oryza sativa* L.). *Environ. Sci. Technol.* **2002**, *36*, 962–968.
(35) Volder, A.; Smart, D. R.; Bloom, A. J.; Eissenstat, D. M. Rapid decline in nitrate uptake and respiration with age in fine lateral roots of grape: Implications for root efficiency and competitive effectiveness. *New Phytol.* **2005**, *165*, 493–501.
(36) Marschner, H. *Mineral Nutrition of Higher Plants*; 2nd ed.; Academic Press: New York, 2003.
(37) Chen, Z.; Zhu, Y. G.; Liu, W. J.; Meharg, A. A. Direct evidence showing the effect of root surface iron plaque on arsenite and arsenate uptake into rice. (*Oryza sativa*) roots. *New Phytol.* **2005**, *165*, 91–97.
(38) Xu, X. Y.; McGrath, S. P.; Zhao, F. J. Rapid reduction of arsenate in the medium mediated by plant roots. *New Phytol.* **2007**, *176*, 590–599.
(39) Kotula, L.; Ranathunge, K.; Schreiber, L.; Steudle, E. Functional and chemical comparison of apoplastic barriers to radial oxygen loss in roots of rice (*Oryza sativa* L.) grown in aerated or deoxygenated solution. *J. Exp. Bot.* **2009**, *60*, 2155–2167.
(40) Mei, X. Q.; Ye, Z. H.; Wong, M. H. The relationship of root porosity and radial oxygen loss on arsenic tolerance and uptake in rice grains and straw. *Environ. Pollut.* **2009**, *157*, 2550–2557.
(41) Tanaka, A.; Loe, R.; Navasero, S. A. Some mechanisms involved in the development of iron toxicity symptoms in the rice plant. *Soil Sci. Plant Nutr.* **1966**, *12*, 32–38.
(42) Blute, N. K.; Brabander, D. J.; Hemond, H. F.; Sutton, S. R.; Newville, M. G.; Rivers, M. L. Arsenic sequestration by ferric iron plaque on cattail roots. *Environ. Sci. Technol.* **2004**, *38*, 6074–6077.
(43) Li, R. Y.; Ago, Y.; Liu, W. J.; Mitani, N.; Feldmann, J.; McGrath, S. P.; Ma, J. F.; Zhao, F. J. The rice aquaporin LSi1 mediates uptake of methylated arsenic species. *Plant Physiol.* **2009**, *150*, 2071–2080.
(44) Pickering, I. J.; Gumaelius, L.; Harris, H. H.; Prince, R. C.; Hirsch, G.; Banks, J. A.; Salt, D. E.; George, G. N. Localizing the biochemical transformations of arsenate in a hyperaccumulating fern. *Environ. Sci. Technol.* **2006**, *40*, 5010–5014.
(45) Pickering, I. J.; Prince, R. C.; George, M. J.; Smith, R. D.; George, G. N.; Salt, D. E. Reduction and coordination of arsenic in Indian mustard. *Plant Physiol.* **2000**, *122*, 1171–1177.
(46) Webb, S. M.; Gaillard, J. F.; Ma, L. Q.; Tu, C. XAS speciation of arsenic in a hyper-accumulating fern. *Environ. Sci. Technol.* **2003**, *37*, 754–760.

ES101139Z